Available online at www.sciencedirect.com
SCIENCE DIRECT®
Microporous and Mesoporous Materials 60 (2003) 197–206
MICROPOROUS AND MESOPOROUS MATERIALS
www.elsevier.com/locate/micromeso

Preparation of Ru metal nanoparticles in mesoporous materials: influence of sulfur on the hydrogenating activity

Peng Tian [a,c], Juliette Blanchard [a,*], Katia Fajerwerg [a], Michèle Breysse [a], Michel Vrinat [b], Zhongmin Liu [c]

[a] *Laboratoire de Réactivité de Surface, UMR CNRS, Université Pierre et Marie Curie, Tour 54-55, 4 place Jussieu, Paris Cedex 05 75252, France*
[b] *Institut de Recherches sur la Catalyse, UPR CNRS, 2 avenue Albert Einstein, 69626 Villeurbanne, France*
[c] *Dalian Institute of Chemical Physics, 457 Zhongshan Road, Dalian 116023, China*

Received 15 October 2002; received in revised form 31 March 2003; accepted 7 April 2003

Abstract

Hydrogenating catalysts were prepared by inserting Ru into the pores of mesoporous Al-MCM-41 materials by selective adsorption of $[Ru(NH_3)_6]^{3+}$. Ru/support catalysts were obtained after reduction with H_2. The activities of these catalysts in hydrogenation reactions were compared to those of Ru/HY and Ru/SiO_2. The catalytic properties in the absence of sulfur were tested in benzene hydrogenation, and the intrinsic activities of all the catalysts (either supported on mesoporous materials or on zeolites) were identical. It was concluded from this result that the dispersion of the Ru metallic phase was similar for all these catalysts. These samples were tested in the tetralin hydrogenation in pure H_2 and in the presence of H_2S (330 ppm of H_2S in H_2). They were found to be much less active than the zeolite-supported catalysts in the presence of H_2S. It is proposed that the lower activity of the catalysts supported on mesoporous materials is either due to their milder acidity, as evidenced by NH_3-TPD, cumene cracking and pyridine desorption experiments, or to the localization of the Ru nanoparticles on alumina islands.

Keywords: Hydrogenation; Mesoporous materials; Ruthenium; Tetralin; Benzene; Acidity

1. Introduction

The hydrogenation of aromatics in diesel fuel is important for both environmental protection and fuel quality. New regulations in Europe and the United States require a reduction of the content of aromatics. At the present time, much research focuses on developing new catalysts and hydrotreating processes in order to meet the gradually stricter diesel fuel specifications. Conventional hydrotreating catalysts containing sulfided mixed oxides (NiMo, NiW and CoMo) can only reach a moderate level of aromatics saturation under typical hydrotreating conditions in a single-state operation [1,2]. Increasing the operation severity does not result in deep levels of aromatics

* Corresponding author. Fax: +33-1-442-76033.
E-mail address: jblanch@ccr.jussieu.fr (J. Blanchard).

1387-1811/03/$ - see front matter © 2003 Elsevier Science Inc. All rights reserved.
doi:10.1016/S1387-1811(03)00377-9

saturation because of thermodynamic limitations. On supported noble metal catalysts, aromatics hydrogenation can be performed at relatively low temperature, i.e. far from the thermodynamic equilibrium. This is the reason why these catalysts perform so well in deep aromatics saturation. The main drawback of these catalysts is that they can be poisoned by small amounts of organic sulfur and nitrogen compounds present in the feed [3,4]. When the noble metal is supported on an acidic zeolite, its sulfur and nitrogen tolerance is greatly improved [5]. According to Dalla Betta and Boudart [6], these variations can be explained by an electron deficiency induced by the interaction between small metal particles and protons of the zeolite. Recent work on Ru metal and sulfide supported on acidic zeolites has evidenced the attractiveness of these catalysts for the hydrogenation of aromatics in the presence of sulfur compounds [7]. However, the use of these catalysts is limited to the conversion of small aromatic molecules due to the pore size of the zeolitic support.

The mesoporous material MCM-41 possesses a hexagonal array of uniform mesopores and a large surface area. Compared to zeolites, only weak and/or medium acid sites exist in Al-MCM-41 [8]. It has been shown that MCM-41 could be a suitable support for preparing noble metal-based catalysts. Song et al. reported that Pt supported on Al-MCM-41 is an active catalyst for the hydrogenation of aromatics in a batch reactor [9]. Corma et al. claimed that platinum-containing MCM-41 can act as a catalyst for the hydrogenation of naphthalene [10]. The authors attributed its excellent activity and sulfur tolerance to the high dispersion of Pt and the interaction of the small Pt clusters with the mildly acidic sites in Al-MCM-41. Therefore, mesoporous silica–alumina materials can be used as an alternative to zeolitic supports for metallic phases.

In this work well dispersed Ru catalysts supported on pure-silica MCM-41 and Al-MCM-41 were prepared and characterized. The acidity strength and the number of Brønsted acid sites were evaluated using ^{27}Al NMR, IR spectroscopy of adsorbed pyridine, temperature-programmed desorption of NH_3 and cumene cracking. The hydrogenating properties of these catalysts were determined in the hydrogenation of tetralin under pure H_2 and under a mixture of H_2 and H_2S (partial pressure of $H_2S = 1.5$ kPa) and compared to the activity of Ru/SiO_2 and Ru/HY_d used as reference catalysts.

2. Experimental

2.1. Preparation of mesoporous materials

The parent pure-silica MCM-41 material was synthesized according to the procedure described by Ryoo et al. [11,12], which includes three pH adjustments at pH = 10 and the addition of NaCl (molar ratio: $NaCl/SiO_2 = 0.75$) during the period of hydrothermal treatment (14 days). A 0.1 M NH_4NO_3 solution in ethanol was used to extract the surfactant from the as-synthesized MCM-41. The ratio of solid/liquid was 1 g/50 cm^3. After a reflux at 358 K for 2 h, the product was filtered, washed, dried at 373 K overnight and then calcined in air (heating from room temperature to 823 K with a rate of 1 K/min followed by 4 h at 823 K).

Al-MCM-41 was prepared by post-synthesis alumination of pure-silica MCM-41 using a method derived from Mokaya and Jones [13]. 25 g $AlCl_3 \cdot 6H_2O$ (99 wt.%, Aldrich) were added to 125 cm^3 distilled water. This solution was heated to 353 K under stirring. 80 cm^3 TMAOH (tetramethyl ammonium hydroxide 10 wt.% in water, Fluka) and 80 cm^3 distilled water were mixed and added to the above solution. After a clear solution was obtained (circa 1 h), 6 g of calcined MCM-41 were added at room temperature under stirring. This mixture was heated to 353 K and kept at this temperature for 2 h. After filtration, washing and drying at 373 K, the product was calcined in air from room temperature to 803 K (1 K/min, 4 h at 803 K).

2.2. Catalyst preparation

The compound used as Ru precursor was $Ru(NH_3)_6Cl_3$ (99.9 wt.%, Johnson & Matthey). Ru supported on MCM-41, Al-MCM-41 and SiO_2

(Aerosil 300 Degussa) were prepared as follows: 1 g of solid was mixed with 40 cm^3 of an aqueous solution of $Ru(NH_3)_6Cl_3$. The pH of the mixture was adjusted using NH_4OH. After equilibration of the solution/silica mixtures under stirring, the solid phase was separated by filtration and washed several times with distilled water to eliminate reversibly adsorbed complexes. This procedure is sometimes called "selective adsorption" in the catalysis literature [14]. Ru supported on HY_d (dealuminated zeolite Y, PQ company) was obtained by ion-exchange as described in [15]. All resulting catalysts were filtered, washed and dried in vacuum at 298 K. Calcination was avoided to prevent the agglomeration of the Ru particles in the presence of O_2, which occurs at relatively low temperature (about 150 °C). The samples were then reduced according to procedures described below.

2.3. Characterization

The contents (wt.%) of Si, Al and Ru in the dried samples were measured by atomic absorption (Central Analysis Service of the CNRS, France).

^{27}Al NMR experiments were run on an MSL300 spectrometer at 78.2 MHz, with a pulse width of 0.7 μs (π/18), a pulse delay of 0.3 s, a spinning rate of 10 kHz and about 3600 scans.

XRD measurements were carried out using a Siemens type D 500 diffractometer with CuKα radiation (wavelength = 1.54 Å). For the mesoporous materials, the scanning range was set between 1.7° and 8° with a step size of 0.02 s.

N_2 adsorption–desorption isotherms were obtained on a Micromeritics ASAP 2010 system at 77 K. Before analysis the supports and catalysts were degassed at 423 and 573 K, respectively, under a pressure of 0.1 Pa for 5 h. The pore sizes were evaluated from the desorption branch of the isotherm using the BJH model.

Transmission FT-IR spectra of adsorbed pyridine were obtained on a Bruker Vector 22 (resolution 2 cm^{-1}, 32 scans/spectrum) spectrometer. A self-supporting wafer of about 4 mg/cm^2 was first calcined under N_2 (100 cm^3/min) in situ in an IR cell at 723 K (0.8 K/min, about 6 h at 723 K) and then evacuated (10^{-4}–10^{-5} mbar) at 723 K for 1 h. Pyridine was admitted to the cell at 298 K, and after 10 min equilibrium, pyridine was desorbed at 298, 423 and 573 K under vacuum (10^{-4}–10^{-5} mbar) during 1 h. All the spectra were recorded at 298 K.

The *temperature-programmed desorption of ammonia* (NH_3-TPD) was carried out with an Autowin 2910 equipment (Micromeritics). The released NH_3 was detected by a mass spectrometer (Omnistar) using the data collected at $e/m = 16$. Ammonia was injected in order to saturate the sample surface at 423 K. Prior to the injection, the sample (100 mg) was activated at 873 K for 40 min (10 K/min) under He (20 cm^3/min). The measurement of the desorbed NH_3 was performed from 423 to 873 K (10 K/min) under He (40 cm^3/min). Because NH_3 decomposes to N_2 and H_2 (at about 573 K) on Ru catalysts, the TPD experiments were only performed on the supports.

2.4. Catalytic activity measurements

Cumene cracking was carried out in a tubular quartz fixed-bed reactor (internal diameter 8 mm) at 573 K in a 25 cm^3/min carrier gas flow of N_2. The catalyst (100 mg) was first activated at 773 K for 2 h (2 K/min) under 25 cm^3/min N_2. Cumene (Aldrich, 99%) vapor was introduced into the reactor by bubbling N_2 through a saturator containing liquid cumene. The cumene flow rate was 11.2 $\mu mol\,min^{-1}$ (partial pressure of cumene 10^3 Pa, WHSV of 3.8 h^{-1}). The products, i.e., benzene and propene were analyzed using an on-line Varian 3800 gas chromatograph with a capillary column.

Benzene hydrogenation was carried out in a fixed-bed microreactor under atmospheric pressure at 323 K. The partial pressure of benzene (99.8%, Merck KGaA, Germany) was kept constant at 6.9×10^3 Pa. The flow rate of H_2 was 100 cm^3/min. The amount of catalyst (circa 50 mg), was chosen such as to obtain a conversion below 10%, where the reaction rate can be calculated using the equation for a differential reaction. The reaction products were separated and identified using an on-line HP 5890 series II gas chromatograph equipped with a capillary column. The only

observed product was cyclohexane. Prior to the activity measurement, each catalyst was pretreated in situ in H_2 (100 cm^3/min) at 773 K for 2 h (3 K/min).

As the catalysts underwent deactivation during the tests, the initial conversion was determined according to a second-order deactivation law [16]: the reciprocal value of the conversion τ versus time t of the run was used to determine the initial conversion τ_0 by extrapolation to zero time:

$$1/\tau = 1/\tau_0 + kt$$

(k is an empirical deactivation constant).

Tetralin hydrogenation was performed in an open high-pressure microreactor working in the gas phase ($P_{H_2} = 4.5$ MPa and $P_{tetralin} = 2.7$ KPa) at 523 K. The total flow rate was 333 cm^3/min. Pure tetralin was introduced into the reactor by means of a gas phase saturator. The products were analyzed by an on-line HP5890 gas chromatograph equipped with a capillary column (HP5.5% phenyl-methyl-silicone, 30 m × 0.53 mm). Because of the slow deactivation of the catalysts, the specific rates were measured after a pseudo-steady-state was reached (around 14 h on stream). High selectivities (>90%) towards hydrogenation products were observed. Small quantities of isomerization products were also detected which were probably methylindanes formed by isomerization of tetralin. The metal catalysts were obtained by reduction in situ under H_2 at 653 K (5 K/min, 5 h at 653 K). After 14 h, 330 ppm H_2S were introduced into the feed in order to investigate the sulfur tolerance of the metal catalyst.

3. Results and discussion

3.1. Catalysts preparation and characterization

Post-synthesis alumination, which allows the insertion of a large amount of Al without collapse of the mesophase, was applied to tune the amount of inserted Al. An Si/Al ratio of 6.3 was obtained in the Al-MCM-41 sample, when a 0.5 mol l^{-1} Al solution was used (Table 1), in agreement with the work of Mokaya and Jones [13].

^{27}Al NMR allows to discriminate between framework tetrahedral (Td) Al ($\delta = 50$ ppm) and extra-framework octahedral (Oh) Al ($\delta = -1$ ppm). The spectra of the Al-MCM-41 sample shown in Fig. 1 do not only display these two peaks but also a third one, located at approximately 30 ppm, which is usually assigned to penta-coordinated Al [17]. ^{27}Al NMR is a semi-quantitative technique, in the sense that part of the Oh Al is NMR-silent due to the high anisotropy of these sites. It is therefore only possible to roughly evaluate the amount of Td Al. By doing so we have found that about 25% of the Al atoms are in tetrahedral positions, i.e. inserted into the silica walls. This rather low value is due to the fact that the number of silanol groups is limited (about 5 Si–OH per nm^2) and part of the aluminum is not

Table 1
Physical properties of different supports and catalysts

Catalyst	Si/Al[a]	Ru (wt.%)[a]	S_{BET} (m^2/g)[b]	APD[c] (Å)	Pore volume (cm^3/g)
MCM-41	–	–	1067	33.9	1.10
Al-MCM-41	6.28 (25)	–	849	32.3	0.86
SiO_2	–	–	223	–	–
HY_d	13.6 (18.5)	–	802 (199)	–	0.24
Ru/MCM-41	–	1.91	507	67.5	0.77
Ru/Al-MCM-41	–	2.07	854	32.4	0.73
Ru/SiO_2	–	1.44	186	–	–
Ru/HY_d	–	1.56	–	–	–

[a] Chemical analysis, the value in the parentheses stands for Si/Al determined by ^{29}Si NMR (HY_d) or estimated from ^{27}Al NMR (Al-MCM-41).

[b] The value in the parentheses stands for the mesopore and external surface area.

[c] APD, average pore diameter (determined using BJH analysis).

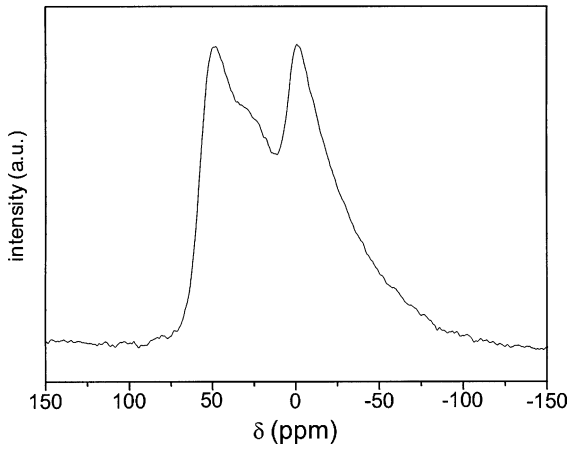

Fig. 1. ^{27}Al MAS NMR spectrum of Al-MCM-41.

inserted into the silica walls and remains octahedrally coordinated at the surface. The framework Si/Al ratio of this sample is higher than that of the reference zeolite (see Table 1). This will result in a lower amount of acid sites and in a lower ion-exchange capacity.

Ruthenium was introduced into the pores using selective adsorption in basic solution. It is well known that the surface charge distribution of oxides is a strong function of the pH of the solution. For silica, the surface is negatively charged above pH 2.5, but the surface charge becomes significant only above 5.0. When the pH exceeds about 10, dissolution of silica occurs [18]. Between pH = 5 and pH = 10 the silanol groups are partly deprotonated, and an ion-exchange reaction between H^+ and the $[Ru(NH_3)_6]^{3+}$ complex occurs. This preparation method permits a high dispersion of the ruthenium phase, due to the strong interaction between the metal complex and the oxide surface. The conditions, depending on the support, are given in Table 2. The amounts of Ru inserted by selective adsorption are reported in Table 2.

XRD and N_2 sorption were used in order to check that the integrity of the support was preserved upon successive addition of Al and Ru. The powder XRD pattern and textural characteristics of the mesoporous MCM-41 support are displayed in Fig. 2a and Table 1. In agreement with Kresge et al. [19], the hexagonal symmetry of the lattice is evidenced by the strong (1 0 0) peak at very low

Table 2
Preparation conditions for the supported ruthenium catalysts

Catalyst	Preparation		
	pH	Ru/support ratio in solution (mmol/g)	Contact time (h)
Ru/MCM-41	7.5	0.4	3
Ru/Al-MCM-41	7.5	0.28	3
Ru/SiO_2	9.0	0.4	16.5
Ru/HY_d	–	0.45	24

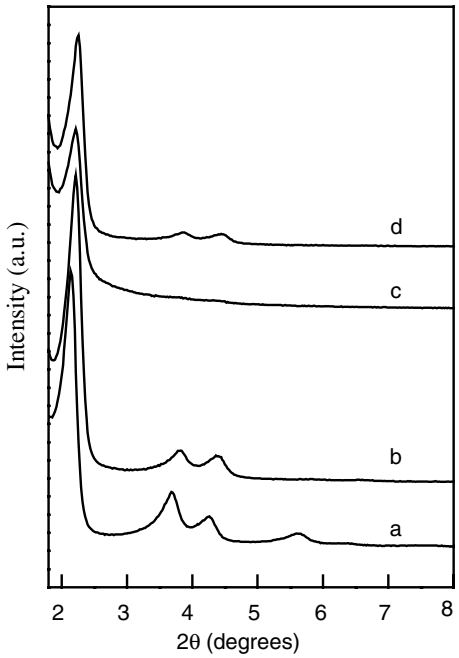

Fig. 2. XRD patterns of mesoporous supports and catalysts. (a) MCM-41; (b) Al-MCM-41; (c) Ru/MCM-41; (d) Ru/Al-MCM-41.

angle and the three weak peaks [(1 1 0), (2 0 0) and (2 1 0)] at comparatively higher angles. The large surface area also agrees with previous works. The evolution of the XRD pattern along the preparation steps is illustrated in Fig. 2 by the diffractograms of MCM-41, Al-MCM-41, Ru/MCM-41 and Ru/Al-MCM-41. The diffraction peaks of the hexagonal structure are still well identified after the introduction of Al, although a minor decrease in the intensities of the high-order peaks can be observed (Fig. 2b). The decrease is intensified for the Ru/Al-MCM-41 samples for which the (2 1 0) diffraction peak is not visible anymore (Fig. 2d).

The most pronounced effect is observed for Ru/MCM-41, for which only the intense peak at low angle is observed (Fig. 2c). This reveals a progressive distortion of the long-range ordering of the hexagonal structure. The latter is associated to a progressive decrease of both the total surface area and pore volume, as shown by the corresponding N_2 physisorption data (Table 1). The increased pore size observed for the Ru/MCM-41 sample is also an indication of the collapse of the pore walls.

Besides the deterioration of structure integrity, the loss of porosity after insertion of Al could be due to increased weights of the samples associated to Al incorporation [13]. When Ru is supported on mesoporous materials, the textural properties of Ru/Al-MCM-41 are only slightly modified, whereas for Ru/MCM-41 its isotherm plot and pore size distribution indicate a loss of its structural integrity (loss of about 50% of the surface area). In accordance with the work of Mokaya and Jone [13], the stability of MCM-41 toward water is enhanced after post-synthesis alumination. Two reasons can be proposed to explain this higher stability. Either a healing of the surface defects of the silica walls due to the consumption of the surface silanol during the alumination step (the incorporation of Al in tetrahedral positions proceeds in solution via the condensation reaction between silanol groups and aluminum), or the formation of a layer of amorphous alumina at the surface of the mesoporous material: due to its higher isoelectric point compared to that of silica, the alumina layer will increase the stability of MCM-41 in mildly basic solutions. For non-porous SiO_2, only a moderate decrease of the surface area is observed after chemical anchoring of ruthenium under more severe pH conditions (see Table 2). The high surface area of ultrastable Y zeolite is also only moderetely decreased by the ion-exchange procedure.

Benzene hydrogenation has been used in order to characterize the dispersion of the Ru phase. This is a structure-insensitive reaction, which means that the activity is proportional to the exposed metallic surface [20,21]. In order to use this reaction to characterize the metallic dispersion, it is necessary to determine the turnover frequency on a catalyst of known dispersion. The dispersion of the Ru phase was determined on Ru/HY_d using TEM. Particle sizes of 1.5–2.5 nm were observed, in agreement with previous work [22]. The mean particle size was 1.8 nm, which corresponds to a metal dispersion of 56%, assuming a cubic shape for the metal particles.

The specific and intrinsic activities of the Ru catalysts are reported in Table 3. The turnover frequency calculated for the Ru/HY_d sample is in agreement with previously published results [23]. However, as proposed by Lin and Vannice [24], the presence of acid sites on this sample might result in a higher hydrogenation activity and therefore a higher TOF than for the catalysts supported on non-acidic (SiO_2 and MCM-41) or mildly acidic (Al-MCM-41) materials. The dispersion of the three other catalysts being evaluated using this value of TOF (see Table 3), one should keep in mind that these values might be underestimated. The dispersions of the metallic phase are similar for all the catalysts (between 46% and 62%) and in agreement with the dispersions reported by Gonzalez et al. [25,26] for Ru dispersed on pure silica using a comparable preparation procedure (see Table 2).The high dispersion of the Ru phase confirms that the preparation method we used is appropriate for the preparation of finely dispersed Ru nanoparticles.

3.2. Acid properties

The acid–base properties of the supports and catalysts were characterized using IR spectroscopy of adsorbed pyridine, cumene cracking and NH_3-TPD.

Table 3
Hydrogenation of benzene at 323 K

Catalyst	$V_s \times 10^6$ (mol g_{cat}^{-1} s^{-1})	$V_i \times 10^2$ (molec s^{-1} $atom_{Ru}^{-1}$)	Dispersion (%)
Ru/HY_d	3.2	2.10	56
Ru/MCM-41	4.4	2.32	62
Ru/Al-MCM-41	3.5	1.72	46
Ru/SiO_2	3.1	2.17	58

Note: Test: $P_{tot} = 0.1$ MPa, $P_{benz} = 6.9$ kPa.

Table 4
B/L acid sites ratio on different supports and catalysts and cumene conversion

Sample	Brønsted/Lewis[a]		Cumene conversion[b] (%)
	423 K	573 K	
Al-MCM-41	0.51	0	45
Ru/Al-MCM-41	0.54	0	36
HY_d	6.67	4.35	92
Ru/HY_d	6.74	4.46	80

[a] Using extinction coefficients by Guisnet et al. [27].
[b] After 2 h time on stream.

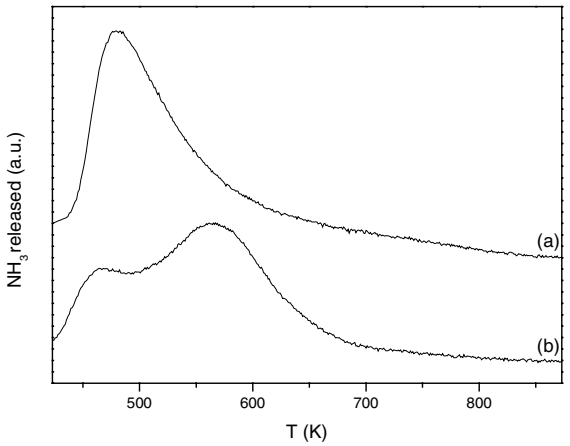

Fig. 3. NH_3-TPD of (a) Al-MCM-41 and (b) HY_d.

Cumene cracking is a well-known probe reaction for Brønsted acidity. Under the conditions used, the reaction proceeded via catalytic cracking (on Brønsted acid sites) to propene and benzene. The cumene conversions obtained by supports and catalysts are given in Table 4. The conversion of Al-MCM-41 is about two times lower than that of HY_d, confirming the presence of acidic sites on this support but also indicating a milder acidity and/or a lower amount of Brønsted sites for the mesoporous support. High conversions are observed for all samples, meaning that the real difference of activity between Al-MCM-41 and HY_d supports might be even higher than the measured one. Moreover, the introduction of ruthenium into the two supports does not significantly modify the distribution of acid sites. Even a slight decrease of cumene conversion is observed. This latter could be explained by the localization and the type of the Ru nanoparticles.

NH_3-TPD was used in order to characterize the strength of the acid sites of the supports (see Fig. 3). Two peaks are expected in the 400–800 K range, namely one at low temperature assigned to the desorption of weakly held ammonia (physisorbed ammonia and ammonia adsorbed on weak Lewis sites) and a second one at higher temperature corresponding to ammonia adsorbed on Brønsted sites. These two peaks overlapped on the desorption curve of Al-MCM-41, giving rise to a broad asymmetric peak centered at 500 K. They are better resolved in the desorption curve of the HY_d zeolite. The overlapping of the two peaks in the curve of Al-MCM-41 is due to the low temperature of ammonia desorption from the Brønsted sites (nearly all the Brønsted sites of this support are free from ammonia at about 550 K) and confirms the milder Brønsted acidity of mesoporous materials compared to zeolites. Due to the presence of weakly bonded ammonia it is not possible to quantify the number of Brønsted sites for the mesoporous support.

The *IR spectra of pyridine* adsorbed on the supports after desorption at 423 and 573 K are shown in Fig. 4. All samples exhibited bands due to the vibration of pyridinium ions adsorbed on Brønsted acid sites (1545 cm^{-1}), coordinated pyridine on Lewis acid sites (1450 cm^{-1}) and pyridine associated with both Brønsted and Lewis sites (1490 cm^{-1}). The ratio Brønsted/Lewis can be estimated using the relative surfaces of the Brønsted and Lewis bands and the molar absorption coefficients of these two sites given by Guisnet et al. [27] ($\epsilon_B = 1.13$, $\epsilon_L = 1.28$ cm μmol^{-1}). The B/L ratio for the supports and the catalysts are displayed in Table 4. After desorption at 423 K, Al-MCM-41 presents a smaller proportion of Brønsted acid sites than the zeolite. The presence of a large amount of Oh Al is responsible of the high intensity of the Lewis band. When the temperature was increased to 573 K, pyridine was desorbed from nearly all the Brønsted acid sites, whereas it remained adsorbed on most Lewis acid sites. For the dealuminated HY_d zeolite, it is obvious that the amount of Brønsted acid sites was higher than that of the Lewis acid sites at 423 K

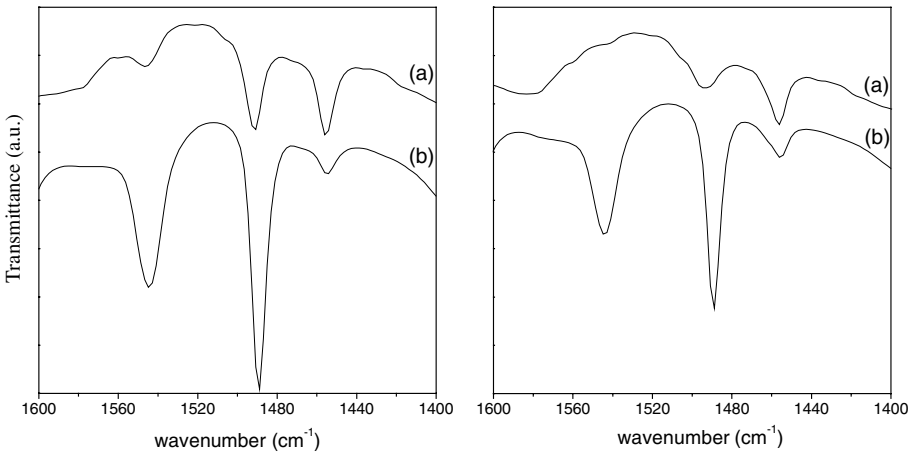

Fig. 4. IR spectra of pyridine adsorbed on catalysts at 423 K (left) and 573 K (right). (a) Al-MCM-41; (b) HY_d.

from Fig. 3. On the other hand, for the zeolite, the distribution of acid sites at 573 K is not significantly modified, except for a slight decrease of the peak intensities. The comparison of the desorption behavior of pyridine on Al-MCM-41 and HY_d confirms the milder acidity of Al-MCM-41 compared to the zeolite. It also confirms, as already noticed in the ^{27}Al NMR and NH_3-TPD studies, that the Al-MCM-41 sample contains a lower amount of Brønsted acid sites. A similar trend was observed for the supported ruthenium catalysts (result not shown).

3.3. Tetralin hydrogenation

In order to investigate the influence of the support on the activity of Ru catalysts in tetralin hydrogenation, reduced catalysts were tested in this reaction with and without H_2S in the reactant feed. The specific rates and the TOFs calculated using the dispersion given in Table 3 are shown in Table 5. Initially, for $p_{H_2S} = 0$ all the catalysts have, as expected, a similar TOF, except Ru/MCM-41. The lower activity for this catalyst might be due to traces of H_2S remaining in the catalytic test device, even for $p_{H_2S} = 0$, that would poison the Ru particles. Indeed, upon addition of 330 ppm H_2S in the feed the activities of all catalysts decrease (Table 5). This decrease is, however, smaller for the Ru/HY_d catalyst than for the three others, indicating that Ru/HY_d possesses a greater sulfur resistance. This is in line with the reported higher resistance towards sulfur of the metallic phase induced by the vicinity of Brønsted acid sites. It has been proposed that the high sulfur tolerance of Ru/HY_d stems from electron-deficient

Table 5
Catalytic activities of supported ruthenium catalysts in tetralin hydrogenation

Catalyst	Specific rate $\times 10^7$ (mol g_{cat}^{-1} s^{-1})			TOF $\times 10^4$ (s^{-1})		
	P_{H_2S}[a] $= 0$	P_{H_2S}[b] $= 330$ ppm	P_{H_2S}[c] $= 0$	P_{H_2S}[a] $= 0$	P_{H_2S}[b] $= 330$ ppm	P_{H_2S}[c] $= 0$
Ru/HY_d	1.8	1.3	–	20.8	15.0	–
Ru/SiO_2	1.6	0.2	0.4	19.3	2.4	4.8
Ru/MCM-41	0.9	0.1	0.4	7.7	0.9	3.4
Ru/Al-MCM-41	2.5	0.1	1.3	26.5	1.1	13.8

Note: Test: 523K, $P_{tot} = 4.5$ MPa, partial pression of tetraline 2.7 kPa.

[a] Activities were measured after around 14 h (when the activity was stable) without H_2S in the feed.

[b] After a, 330 ppm H_2S were introduced into the feed and the activity was measured after around 2 h.

[c] After b, H_2S in the feed was removed and the activity was measured after around 4 h.

$Ru^{\delta+}$. According to Sachtler and coworkers [28,29], a metal-proton adduct could be formed between the metal and Brønsted acid sites of the zeolite, which would lower the strength of the Ru–S bond, thus enhancing the S-tolerance of the catalyst. However, one would also expect a higher sulfur resistance of the metallic phase supported on Al-MCM-41. The fact that the poisoning of the metallic sites is similar on acidic and non-acidic mesoporous materials tends to indicate that either the acidity of these materials is too low to bring about sulfur resistance of the metallic phase or the Ru nanoparticles are not located in the vicinity of these acidic sites. The ^{27}Al NMR study has indeed evidenced the presence of a large amount of Oh Al that could form islands of amorphous alumina at the surface of the silica walls, where the Ru nanoparticles could be located. This would prevent the expected effect of the acid sites. Corma et al. have reported, in contrast with the first hypothesis, that Pt-containing Al-MCM-41, MSA (mesoporous amorphous silica–alumina) and ASA (amorphous silica–alumina) possessed similar acidity, but that Pt/Al-MCM-41 presented a higher sulfur tolerance comparable to the one of Pt/USY [10]. However, no similar study has yet been performed on Ru nanoparticles.

Upon removal of H_2S from the feed, the activity was restored to some extent depending on the support. The activities measured 4 h after the removal of H_2S indicate that the restoring ability is about 50% (Table 5). This means that part of the poisoning occurring in the presence of H_2S is reversible in a pure H_2 atmosphere.

Preliminary results performed on sulfided catalysts have evidenced a similar trend, confirming that the activity of Ru metal or sulfide for the hydrogenation of aromatics in the presence of sulfur is higher when the strength of acid sites is higher [15].

4. Conclusion

This work demonstrates that mesoporous materials are suitable supports for the preparation of well dispersed supported Ru catalysts. The characterization of the acidity (strength and number of acid sites) of Al-MCM-41 confirms that the Brønsted acidity in this material is milder than in zeolites. The number of acid sites was also shown to be smaller than in the reference zeolite. This result, associated with the presence of a large number of Lewis sites indicates that a large portion of the Al is in octahedral positions. This could result in the formation of alumina island at the surface of the silica walls.

All the samples exhibit similar specific activities in benzene and tetralin hydrogenation (without H_2S in the feed) indicating that the dispersion of the Ru phase is similar for all the catalysts. Upon addition of H_2S to the feed, a tremendous decrease of reactivity is observed for all the samples except the zeolite. This result is expected for non-acidic supports (silica and MCM-41). However, the unexpectedly low sulfur resistance of Al-MCM-41 can be ascribed either to the too mild Brønsted acidity of this support or to the localization of the Ru particles on alumina islands.

In the future, the too low activity of Ru/Al-MCM-41 catalysts could be overcome either by increasing the acidity strength of the Al lattice sites or by decreasing the amount of Al extra-lattice species. It is indeed possible to increase the acidity of the mesoporous materials by using new preparation techniques, as described in Refs. [30,31]. On the other hand, the formation of amorphous alumina at the surface of the silica wall can be prevented by changing the preparation conditions and especially by reducing the amount of Al in the alumination solution [13].

Acknowledgements

This work has been carried out within the frame of the French-Chinese collaboration on catalysis (PRA n°E00 02 and LFCC). J. Maquet is gratefully acknowledged for ^{27}Al NMR measurements and M. Cattenot for catalytic tests.

References

[1] B.H. Cooper, B.B.L. Donnis, Appl. Catal. A: Gen. 137 (1996) 203–223.
[2] A. Stanislaus, B.H. Cooper, Catal. Rev. Sci. Eng. 36 (1994) 75–123.

[3] C.H. Bartholomew, P.K. Agrawal, J.R. Katzer, in: D.D. Eley, H. Pines, P.B. Weisz (Eds.), Advances in Catalysis, vol. 31, Academic Press, New York, 1982, pp. 135–242.
[4] J. Barbier, E. Lamy-Pitara, P. Marecot, J.P. Boitiaux, J. Cosyns, F. Verna, in: D.D. Eley, H. Pines, P.B. Weisz (Eds.), Advances in Catalysis, vol. 37, Academic Press, San Diego, California, 1990, pp. 279–318.
[5] A. Arcoya, A. Cortes, J.L.G. Fierro, X.L. Seoane, in: C.H. Bartholomew, J.B. Butt (Eds.), Catalyst Deactivation, 1991: Proceedings of the 5th International Symposium, Studies in Surface Science and Catalysis, vol. 68, Elsevier, Amsterdam, 1991, pp. 557–564.
[6] R.A. Dalla Betta, M. Boudart, Catal., Proc. Int. Congr., 5th 2 (1973) 1329–1341.
[7] M. Breysse, M. Cattenot, V. Kougionas, J.C. Lavalley, F. Mauge, J.L. Portefaix, J.L. Zotin, J. Catal. 168 (1997) 143–153.
[8] B. Chakraborty, B. Viswanathan, Catal. Today 49 (1999) 253–260.
[9] K.M. Reddy, C.S. Song, Catal. Today 31 (1996) 137–144.
[10] A. Corma, A. Martinez, V. Martinezsoria, J. Catal. 169 (1997) 480–489.
[11] R. Ryoo, J.M. Kim, C.H. Ko, in: L. Bonneviot, F. Belard, C. Danumah, S. Giasson, S. Kaliaguine (Eds.), Mesoporous Molecular Sieves 1998, Studies in Surface Science and Catalysis, vol. 117, Elsevier, Amsterdam, 1998, pp. 151–158.
[12] J.M. Kim, S. Jun, R. Ryoo, J. Phys. Chem. B 103 (1999) 6200–6205.
[13] R. Mokaya, W. Jones, J. Mater. Chem. 9 (1999) 555–561.
[14] J.F. Lambert, M. Che, in: G. Centi (Ed.), Catalysis by Unique Metal Ion Structures in Solid Matrices, NATO Science Series, II: Mathematics, Physics and Chemistry, vol. 13, Kluwer Academic Publishers, Utrecht, 2001, pp. 1–19.
[15] C. Sun, M.-J. Peltre, M. Briend, J. Blanchard, K. Fajerwerg, J.-M. Krafft, M. Breysse, M. Cattenot, M. Lacroix, Appl. Catal. A: Gen., in press.
[16] O. Levenspiel, J. Catal. 25 (1972) 265–272.
[17] H. Kosslick, G. Lischke, B. Parlitz, W. Storek, R. Fricke, Appl. Catal. A: Gen. 184 (1999) 49–60.
[18] R.K. Iler, The Chemistry of Silica, Wiley-Interscience, New York, 1979, pp. 30–49.
[19] C.T. Kresge, M.E. Leonowicz, W.J. Roth, J.C. Vartuli, J.S. Beck, Nature (London) 359 (1992) 710–712.
[20] M. Boudart, A. Aldag, J.E. Benson, N.A. Dougharty, C.G. Harkins, J. Catal. 6 (1966) 92–99.
[21] M. Boudart, Advan. Catal. Relat. Subject 20 (1969) 153–166.
[22] B. Moraweck, G. Bergeret, M. Cattenot, V. Kougionas, C. Geantet, J.-L. Portefaix, J.L. Zotin, M. Breysse, J. Catal. 165 (1997) 45–56.
[23] B. Coughlan, S. Narayanan, W.A. McCann, M. Carroll, J. Catal. 49 (1977) 97–108.
[24] S.D. Lin, M.A. Vannice, J. Catal. 143 (1993) 539–553.
[25] W. Zou, R.D. Gonzalez, J. Catal. 133 (1992) 202–219.
[26] R.D. Gonzalez, H. Miura, Catal. Rev. Sci. Eng. 36 (1994) 145–177.
[27] M. Guisnet, P. Ayrault, C. Coutanceau, M.F. Alvarez, J. Datka, J. Chem. Soc. Faraday Trans. 93 (1997) 1661–1665.
[28] W.M.H. Sachtler, A.Y. Stakheev, Catal. Today 12 (1992) 283–295.
[29] W.M.H. Sachtler, Z. Zhang, in: D.D. Eley, H. Pines, P.B. Weisz (Eds.), Advances in Catalysis, vol. 39, Academic Press, San Diego, California, 1993, pp. 129–220.
[30] Z.T. Zhang, Y. Han, L. Zhu, R.W. Wang, Y. Yu, S.L. Qiu, D.Y. Zhao, F.S. Xiao, Angew. Chem. Inter. Edit. 40 (2001) 1258–1262, 1151.
[31] D.T. On, S. Kaliaguine, Angew. Chem. Inter. Edit. 40 (2001) 3248–3251.